Measurement of A_c with charmed mesons at the SLAC Large Detector

Kenji Abe,[15] Koya Abe,[24] T. Abe,[21] I. Adam,[21] H. Akimoto,[21] D. Aston,[21] K. G. Baird,[11] C. Baltay,[30] H. R. Band,[29] T. L. Barklow,[21] J. M. Bauer,[12] G. Bellodi,[17] R. Berger,[21] G. Blaylock,[11] J. R. Bogart,[21] G. R. Bower,[21] J. E. Brau,[16] M. Breidenbach,[21] W. M. Bugg,[23] D. Burke,[21] T. H. Burnett,[28] P. N. Burrows,[17] A. Calcaterra,[8] R. Cassell,[21] A. Chou,[21] H. O. Cohn,[23] J. A. Coller,[4] M. R. Convery,[21] V. Cook,[28] R. F. Cowan,[13] G. Crawford,[21] C. J. S. Damerell,[19] M. Daoudi,[21] S. Dasu,[29] N. de Groot,[2] R. de Sangro,[8] D. N. Dong,[21] M. Doser,[21] R. Dubois,[21] I. Erofeeva,[14] V. Eschenburg,[12] E. Etzion,[29] S. Fahey,[5] D. Falciai,[8] J. P. Fernandez,[26] K. Flood,[11] R. Frey,[16] E. L. Hart,[23] K. Hasuko,[24] S. S. Hertzbach,[11] M. E. Huffer,[21] X. Huynh,[21] M. Iwasaki,[16] D. J. Jackson,[19] P. Jacques,[20] J. A. Jaros,[21] Z. Y. Jiang,[21] A. S. Johnson,[21] J. R. Johnson,[29] R. Kajikawa,[15] M. Kalelkar,[20] H. J. Kang,[20] R. R. Kofler,[11] R. S. Kroeger,[12] M. Langston,[16] D. W. G. Leith,[21] V. Lia,[13] C. Lin,[11] G. Mancinelli,[20] S. Manly,[20] G. Mantovani,[18] T. W. Markiewicz,[21] T. Maruyama,[21] A. K. McKemey,[3] R. Messner,[21] K. C. Moffeit,[21] T. B. Moore,[30] M. Morii,[21] D. Muller,[21] V. Murzin,[14] S. Narita,[24] U. Nauenberg,[5] H. Neal,[30] G. Nesom,[17] N. Oishi,[15] D. Onoprienko,[23] L. S. Osborne,[13] R. S. Panvini,[27] C. H. Park,[22] I. Peruzzi,[8] M. Piccolo,[8] L. Piemontese,[7] R. J. Plano,[20] R. Prepost,[29] C. Y. Prescott,[21] B. N. Ratcliff,[21] J. Reidy,[12] P. L. Reinertsen,[26] L. S. Rochester,[21] P. C. Rowson,[21] J. J. Russell,[21] O. H. Saxton,[21] T. Schalk,[26] B. A. Schumm,[26] J. Schwiening,[21] V. V. Serbo,[21] G. Shapiro,[10] N. B. Sinev,[16] J. A. Snyder,[30] H. Staengle,[6] A. Stahl,[21] P. Stamer,[20] H. Steiner,[10] D. Su,[21] F. Suekane,[24] A. Sugiyama,[15] S. Suzuki,[15] M. Swartz,[9] F. E. Taylor,[13] J. Thom,[21] E. Torrence,[13] T. Usher,[21] J. Va'vra,[21] R. Verdier,[13] D. L. Wagner,[5] A. P. Waite,[21] S. Walston,[16] A. W. Weidemann,[23] E. R. Weiss,[28] J. S. Whitaker,[4] S. H. Williams,[21] S. Willocq,[11] R. J. Wilson,[6] W. J. Wisniewski,[21] J. L. Wittlin,[11] M. Woods,[21] T. R. Wright,[29] R. K. Yamamoto,[13] J. Yashima,[24] S. J. Yellin,[25] C. C. Young,[21] and H. Yuta[1]

(The SLD Collaboration)

[1]*Aomori University, Aomori, 030 Japan*
[2]*University of Bristol, Bristol, United Kingdom*
[3]*Brunel University, Uxbridge, Middlesex, UB8 3PH United Kingdom*
[4]*Boston University, Boston, Massachusetts 02215*
[5]*University of Colorado, Boulder, Colorado 80309*
[6]*Colorado State University, Ft. Collins, Colorado 80523*
[7]*INFN Sezione di Ferrara and Universita di Ferrara, I-44100 Ferrara, Italy*
[8]*INFN Lab. Nazionali di Frascati, I-00044 Frascati, Italy*
[9]*Johns Hopkins University, Baltimore, Maryland 21218-2686*
[10]*Lawrence Berkeley Laboratory, University of California, Berkeley, California 94720*
[11]*University of Massachusetts, Amherst, Massachusetts 01003*
[12]*University of Mississippi, University, Mississippi 38677*
[13]*Massachusetts Institute of Technology, Cambridge, Massachusetts 02139*
[14]*Institute of Nuclear Physics, Moscow State University, 119899, Moscow, Russia*
[15]*Nagoya University, Chikusa-ku, Nagoya, 464 Japan*
[16]*University of Oregon, Eugene, Oregon 97403*
[17]*Oxford University, Oxford, OX1 3RH, United Kingdom*
[18]*INFN Sezione di Perugia and Universita di Perugia, I-06100 Perugia, Italy*
[19]*Rutherford Appleton Laboratory, Chilton, Didcot, Oxon OX11 0QX, United Kingdom*
[20]*Rutgers University, Piscataway, New Jersey 08855*
[21]*Stanford Linear Accelerator Center, Stanford University, Stanford, California 94309*
[22]*Soongsil University, Seoul, 156-743, Korea*
[23]*University of Tennessee, Knoxville, Tennessee 37996*
[24]*Tohoku University, Sendai 980, Japan*
[25]*University of California at Santa Barbara, Santa Barbara, California 93106*
[26]*University of California at Santa Cruz, Santa Cruz, California 95064*
[27]*Vanderbilt University, Nashville, Tennessee 37235*
[28]*University of Washington, Seattle, Washington 98105*
[29]*University of Wisconsin, Madison, Wisconsin 53706*
[30]*Yale University, New Haven, Connecticut 06511*

(Received 13 September 2000; published 9 January 2001)

We present a direct measurement of the parity-violation parameter A_c in the coupling of the Z^0 to c quarks with the SLD detector. The measurement is based on a sample of 530 k hadronic Z^0 decays, produced with a mean electron-beam polarization of $|P_e| = 73\%$. The tagging of c-quark events is performed using two methods: the exclusive reconstruction of D^{*+}, D^+, and D^0 mesons, and the soft pions (π_s) produced in the decay

of $D^{*+}\to D^0\pi_s^+$. The large background from D mesons produced in B hadron decays is separated efficiently from the signal using precision vertex information. The combination of these two methods yields $A_c=0.688\pm0.041$.

DOI: 10.1103/PhysRevD.63.032005 PACS number(s): 13.38.Dg, 11.30.Er, 12.15.Ji, 14.65.Dw

I. INTRODUCTION

In the standard model, the Z^0 coupling to fermions has both vector (v_f) and axial-vector (a_f) components. Measurements of fermion asymmetries at the Z^0 resonance probe a combination of these components given by

$$A_f=2v_fa_f/(v_f^2+a_f^2). \tag{1}$$

The parameter A_f expresses the extent of parity violation at the $Zf\bar{f}$ vertex and its measurement provides a sensitive test of the standard model.

At the Born level, the differential cross section for the reaction $e^+e^-\to Z^0\to f\bar{f}$ is

$$\sigma_f(z)\equiv d\sigma_f/dz\propto(1-A_eP_e)(1+z^2)+2A_f(A_e-P_e)z, \tag{2}$$

where P_e is the longitudinal polarization of the electron beam ($P_e>0$ for net right-handed polarization) and $z=\cos\theta$, θ being the polar angle of the outgoing fermion relative to the incident electron. In the absence of electron beam polarization, the parameter A_f can be extracted by isolating the term linear in z via the forward-backward asymmetry:

$$A_{FB}^f(z)=\frac{\sigma^f(z)-\sigma^f(-z)}{\sigma^f(z)+\sigma^f(-z)}=A_eA_f\frac{2z}{1+z^2}, \tag{3}$$

which also depends on the initial state electron parity-violation parameter A_e. At the SLAC Linear Collider (SLC), the ability to manipulate the longitudinal polarization of the electron beam allows the isolation of the parameter A_f in Eq. (2), independent of A_e, using the left-right forward-backward asymmetry:

$$\tilde{A}_{FB}^f(z)=\frac{[\sigma_L^f(z)-\sigma_L^f(-z)]-[\sigma_R^f(z)-\sigma_R^f(-z)]}{[\sigma_L^f(z)+\sigma_L^f(-z)]+[\sigma_R^f(z)+\sigma_R^f(-z)]}$$
$$=|P_e|A_f\frac{2z}{1+z^2}, \tag{4}$$

where indices L, R refers to $Z^0\to f\bar{f}$ decays produced with left-handed or right-handed polarization of the electron beam, respectively. For a highly polarized electron beam with $|P_e|=73\%$, $\tilde{A}_{FB}^f$ provides a statistical advantage of $(P_e/A_e)^2\sim24$ in the sensitivity to A_f relative to the unpolarized asymmetry.

In this paper, we present a direct measurement of the parity-violation parameter A_c for the $Zc\bar{c}$ coupling. The c quark[1] is the only up-type quark which can be identified, and its measurements provides sensitive test of the standard model. The tagging of c quarks is performed using exclusively reconstructed D^{*+}, D^+, and D^0 mesons, as well as an inclusive sample of $D^{*+}\to D^0\pi_s^+$ decays identified by the soft-pion (π_s).

The charge of the primary c quark is determined by the charge of the $D^{(*)}$, K (in the D^0 reconstruction case), or π_s (in the soft-pion analysis case). The direction of the primary quark is estimated from the direction of the exclusively reconstructed $D^{(*)+}$ or D^0 meson, or the jet axis in the soft-pion analysis. The value of A_c is extracted via an unbinned maximum likelihood fit. The fit is performed on two separate data samples: one collected between 1993 and 1995, and the other, with an improved vertex detector, between 1996 and 1998. The data samples associated with these two periods comprise 150 k and 380 k hadronic Z^0 decays, respectively.

The measurement of A_c presented in this paper updates and supersedes our previous publication [1], which was based on a sample of 50 k hadronic Z^0 decays from 1993 alone. There are several direct and indirect A_c measurements [1–3]. The measurement reported here is currently the most precise.

II. APPARATUS AND EVENT SELECTION

The measurement described here is based on 530 k hadronic Z^0 decays recorded in 1993–1998 with the SLC Large Detector (SLD) at the SLC e^+e^- collider at a mean center-of-mass-energy of 91.27 GeV(1993–1995) or 91.24 GeV(1996–1998). A general description of the SLD can be found elsewhere [4]. Charged-particle tracking for the 1993–1995 data sample uses the central drift chamber (CDC) [5] and VXD2 [6] CCD pixel vertex detector. For this system, the measured impact-parameter resolution in the transverse (longitudinal) direction with respect to the beam axis can be approximated by $11\oplus70/P\sin^{5/2}\theta$ μm ($38\oplus70/P\sin^{5/2}\theta$ μm), as a function of the track momentum P (in GeV/c) and the polar angle θ. In 1996, we installed the upgraded 307M pixel vertex detector (VXD3) [7], which provides improved impact-parameter resolution of $7.8\oplus33/P\sin^{5/2}\theta$ μm ($9.7\oplus33/P\sin^{5/2}\theta$ μm) [8] in the transverse (longitudinal) direction with respect to the beam axis. In addition, VXD3 extended the polar-angle coverage from $|\cos\theta|<0.75$ to $|\cos\theta|<0.85$. Combining the CDC and the VXD, a momentum resolution of $\sigma(P_T)/P_T=\sqrt{(0.01)^2+(0.0026P_T/\mathrm{GeV})^2}$ is achieved. The Liquid Argon Calorimeter (LAC) [9] measures the energy of charged

[1]Throughout the paper charge-conjugate states are implicitly included.

and neutral particles and is also used for electron identification. The barrel LAC covers the polar-angle region of $|\cos\theta|<0.84$, and has energy resolutions of $15\%/\sqrt{E(\mathrm{GeV})}$ and $65\%/\sqrt{E(\mathrm{GeV})}$ for electromagnetic and hadronic showers, respectively. Muon identification is provided by the Warm Iron Calorimeter (WIC) [10]. The Čerenkov Ring Imaging Detector (CRID) [11] provides particle identification. In order to achieve particle identification over a wide momentum range, the CRID uses two different radiator systems; liquid (C_6F_{14}) and gas (C_5F_{12}), which provide excellent π/K separation in the momentum range from 0.3 to 35 GeV/c.

The SLC operates a polarized electron beam and an unpolarized positron beam [12]. The average electron polarization measured for the 1993–1998 data sample is $|P_e|=73\pm0.5\%$ [12,13]. The SLC interaction-point (IP) size in the xy plane is 2.6 μm$\times$0.8 μm and its mean position is reconstructed with a precision of $\sigma_{IP}=4\,\mu$m (7 μm) using the tracks in sets of $\sim$30 sequential hadronic events for the 1996–1998 (1993–1995) data sets [14]. The event-by-event median z position of tracks at their point of closest approach to the IP in the xy plane determines the z position of the Z^0 primary vertex (PV) with a precision of $\sim$15 μm (35 μm) for the 1996–1998 (1993–1995) data.

Hadronic events are selected by requiring at least 5 charged tracks, a total charged energy of at least 20 GeV/c, and a thrust axis calculated from charged tracks satisfying $|\cos\theta_{thrust}|<0.87$ (0.8 for the 1993–1995 data). In the event selection and charm reconstruction, we use the quality tracks which satisfy the following criteria for the 1996–1998 (1993–1995) samples:

(1) At least 23 (30 for the 1993–1995 data) associated CDC hits;

(2) A radius of the innermost CDC hit of the reconstructed track within 50 cm (39 cm) of the IP;

(3) An xy and rz impact parameter with respect to the IP of less than 5 cm (10 cm);

(4) A reconstructed polar angle θ within $|\cos\theta|<0.87$ (0.80); and

(5) A momentum component transverse to the beam axis greater than 0.15 GeV/c.

As $Z^0\to b\bar{b}$ events are also a copious source of D mesons, they represent a potential background. We reject these events using the invariant mass of the charged tracks associated with the reconstructed secondary decay vertices [15]. In particular, we require that there must be no vertex with invariant mass greater than 2.0 GeV/c^2. Monte Carlo (MC) simulations indicate that this cut rejects 57% of $b\bar{b}$ events while preserving 99% of $c\bar{c}$ events.

III. A_c MEASUREMENT WITH EXCLUSIVE CHARMED-MESON RECONSTRUCTION

In this analysis, we reconstruct three different $D^{(*)}$ meson states for c-quark tagging: the pseudoscalar mesons D^+ and D^0, and the vector meson D^{*+}. This section describes the procedure for their reconstruction, as well as the corresponding A_c measurement and a discussion of associated systematic errors.

A. D^{*+} selection

D^{*+} mesons are identified via the decay $D^{*+}\to D^0\pi_s^+$ followed by

$$D^0\to K^-\pi^+ \quad K\pi,$$

$$D^0\to K^-\pi^+\pi^0 \quad \text{satellite},$$

$$D^0\to K^-\pi^+\pi^-\pi^+ \quad K\pi\pi\pi, \text{ or}$$

$$D^0\to K^-l^+\nu_l \quad (l=\mathrm{e} \text{ or } \mu) \quad \text{semileptonic}.$$

In these decays, the charge of the underlying c quark is specified by the charge of the ''soft pion'' π_s. No attempt is made to reconstruct the π^0 in the satellite mode, nor to estimate the neutrino direction or energy in the semileptonic mode.

We search for D^{*+} mesons in each of the two event hemispheres, defined by the plane perpendicular to the thrust axis, using all quality tracks with at least one hit in the VXD. In the $K\pi\pi\pi$ mode, we only use tracks which have momentum greater than 0.75 GeV/c. We first construct D^0 candidates using all combinations of tracks corresponding to the charged multiplicity in each D^0 decay mode, with zero net charge. Here one of them is assigned the charged kaon mass and the other(s) are assigned the charged pion mass. In the semileptonic mode, we combine an identified electron or muon track with another track which has opposite charge and assume the track to be a kaon. Electrons are identified based on the momentum measured with the CDC and the energy deposited in the calorimeter [16]. Electrons from γ-conversions are rejected. Muon candidates are identified by the association of extrapolated CDC tracks with hits in the WIC [16].

A vertex fit is performed on the tracks forming a D^0 candidate, and we require that its χ^2 probability be greater than 1%. The invariant mass M of the D^0 candidates is required to lie within the following ranges:

$$1.765\ \mathrm{GeV}/c^2<M_{D^0}<1.965\ \mathrm{GeV}/c^2 \quad (K\pi),$$

$$1.500\ \mathrm{GeV}/c^2<M_{D^0}<1.600\ \mathrm{GeV}/c^2 \quad (\text{satellite}),$$

$$1.795\ \mathrm{GeV}/c^2<M_{D^0}<1.935\ \mathrm{GeV}/c^2 \quad (K\pi\pi\pi),$$

$$1.100\ \mathrm{GeV}/c^2<M_{D^0}<1.800\ \mathrm{GeV}/c^2 \quad (\text{semileptonic}).$$

These reconstructed pseudoscalar meson candidates are then combined with a soft-pion candidate track with charge opposite to that of the kaon candidate, thus forming the D^{*+} candidate.

To reconstruct the D^{*+}, we use two sets of selection criteria. One is based on event kinematics and the other on event topology. The former relies on the fact that D^{*+} me-

sons in $c\bar{c}$ events have much higher $x_{D^*}\equiv 2E_{D^*}/E_{CM}$, where E_{D^*} is the D^{*+} energy, than those in $b\bar{b}$ events or random combinatoric background (RCBG). The latter relies on the fact that D^0's in $c\bar{c}$ events have a longer 3D decay length (~ 1 mm) than that for RCBG, and originate at the primary vertex, in contrast to those D^0's in $b\bar{b}$ events emerging from B decay vertices. We select the combinations which satisfy either condition.

In the selection based on the event kinematics, we require the candidate to have x_{D^*} greater than 0.4 ($K\pi$, satellite, and semileptonic) or 0.6 ($K\pi\pi\pi$). For a true D^0 candidate, the distribution of $\cos\theta^*$, where θ^* is the opening angle between the direction of the D^0 in the laboratory frame and the kaon in the D^0 rest frame, is expected to be flat. Since background events peak at $\cos\theta^*=\pm 1$, they are further reduced by requiring $|\cos\theta^*|\leq 0.9$ ($K\pi$, satellite, and semileptonic) or 0.8 ($K\pi\pi\pi$). We also require the soft-pion candidate to have momentum greater than 1 GeV/c. In the satellite mode, we apply a 3D decay-length cut of $L/\sigma_L>1.5$ on the reconstructed D^0 vertices to reduce the RCBG. (The average decay-length resolution is $\langle\sigma_L\rangle\sim 150$ μm.)

In the selection based on the event topologies, we require the reconstructed D^0 vertices to have 3D decay-length significance $L/\sigma_L>2.5$, and the xy impact parameter of the D^0 momentum vector to the IP to be less than 20 μm ($K\pi$ and $K\pi\pi\pi$) or 30 μm (satellite and semileptonic). The latter cut is effective in rejecting D decays in $b\bar{b}$ events. Since these D's have significant P_T relative to the parent B flight direction, and the B's themselves have a significant flight length (~ 3.5 mm), many of these D's do not appear to originate from the primary vertex. A cut of x_{D^*} greater than 0.3 ($K\pi$, satellite, and semileptonic) or 0.4 ($K\pi\pi\pi$) is also applied. Figure 1 shows the distribution of xy impact parameter of the D^0 relative to the IP for the decay of $D^{*+}\rightarrow D^0\pi_s^+$, $D^0\rightarrow K^-\pi^+$. In this figure, we do not reject B-decay candidate events with the invariant mass cut of the reconstructed secondary vertices described above, only for the purpose of showing how the xy-impact-parameter cut is effective in rejecting the B-decay background. After applying the invariant mass cut of the reconstructed secondary vertices, 34% of the remaining B-decay background events are rejected by the xy-impact-parameter cut.

The overlaps of the sets of candidates from the event kinematics and topology analysis are 53% ($K\pi$), 50% (satellite), 28% ($K\pi\pi\pi$), and 36% (semileptonic). In the $K\pi\pi\pi$ sample, there may be multiple D^0 candidates in a single event which pass the above cuts. To avoid double counting and to reduce the background, we select the D^0 candidate with the lowest vertex χ^2.

Having selected a candidate, we form the mass difference $\Delta M=M_{D^*}-M_{D^0}$. The mass difference spectra for the four reconstructed D^{*+} decay modes are shown in Fig. 2. For all decay modes, clear peaks around $\Delta M=0.14$ GeV/c^2 appear due to the D^{*+} to D^0 transition. We include the candidates in the signal sample provided ΔM is less than 0.148 GeV/c^2 ($K\pi$ and $K\pi\pi\pi$), less than 0.155 GeV/c^2 (satellite), and less than 0.16 GeV/c^2 (semileptonic). The

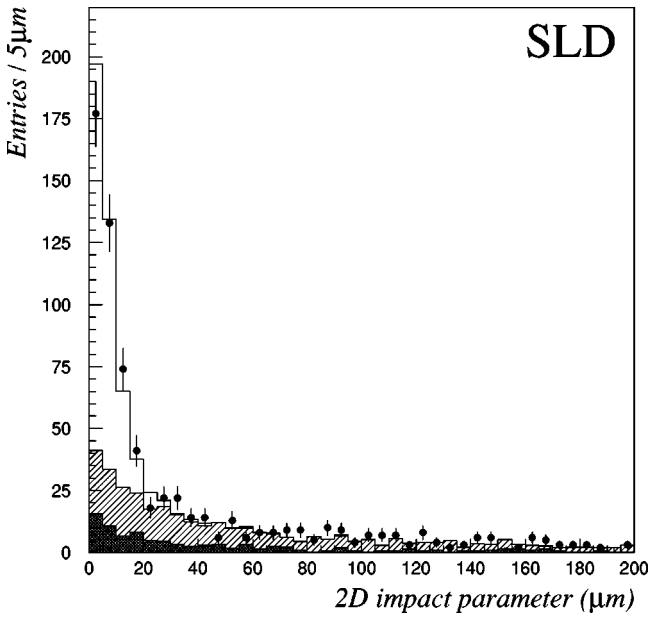

FIG. 1. The distribution of the 2D impact parameter of the D^0 momentum vector to the IP for the decay of $D^{*+}\rightarrow D^0\pi_s^+$, $D^0\rightarrow K^-\pi^+$. The solid circles indicate the experimental data, and histograms are MC of D^{*+} from c quark (open), from b quark (single hatched), and RCBG (double hatched).

side-band region is defined as $0.16<\Delta M<0.20$ GeV/c^2 ($0.17<\Delta M<0.20$ GeV/c^2 for the semileptonic mode), and is used to estimate the RCBG contamination in the signal region. In the figure, the MC predictions for the reconstructed D^{*+} (open) and RCBG (hatched) are also presented. For the MC prediction, the relative normalizations of signal and RCBG shapes are adjusted so that the predicted numbers of events match those observed in the data signal and side-band regions. Averaged over the various modes, this procedure requires adding 10% to the MC signal and 5% to the MC RCBG. The number of the selected candidates as well as the contributions of $c,b\rightarrow D$ and RCBG estimated by MC are summarized in Table I.

B. D^+ and D^0 selection

The D^+ and D^0 mesons are identified via the decay channels

$$D^+\rightarrow K^-\pi^+\pi^+$$

$$D^0\rightarrow K^-\pi^+.$$

These modes are reconstructed by considering all quality tracks in each hemisphere which have VXD hits. In the D^+ reconstruction, we additionally require each track to have a momentum of greater than 1 GeV/c.

For the D^+ reconstruction, we combine two same-sign tracks, assumed to be pions, with an opposite-sign track, assumed to be a kaon. We require that x_{D^+} be greater than 0.4, and $\cos\theta^*$ be greater than -0.8, where θ^* is the opening angle between the direction of the D^+ in the laboratory frame and the kaon in the D^+ rest frame. To reject D^{*+}

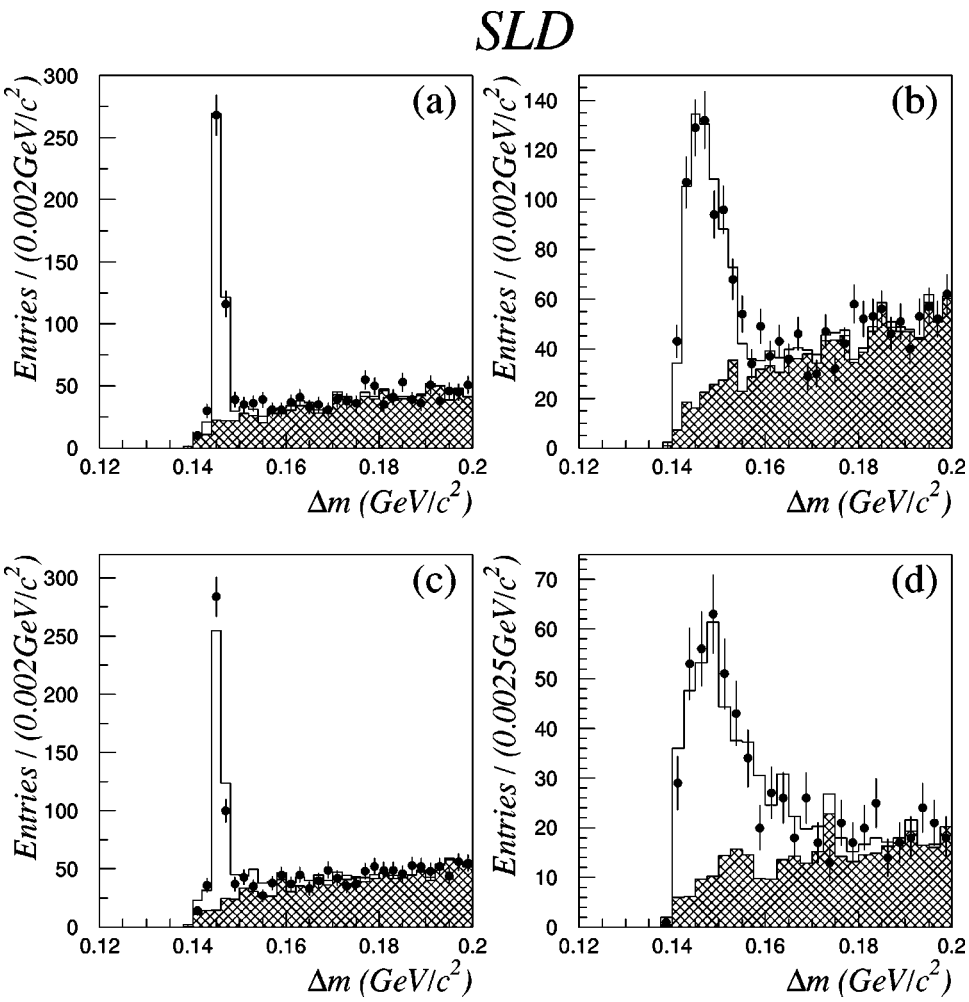

FIG. 2. The mass-difference distributions for the decay of (a) $D^{*+}\to D^0\pi_s^+$, $D^0\to K^-\pi^+$, (b) $D^0\to K^-\pi^+\pi^0$, (c) $D^0\to K^-\pi^+\pi^+\pi^-$, and (d) $D^0\to K^-l^+\nu_l$ (l=e or μ). The solid circles indicate the experimental data, and histograms are MC of signal (open) and RCBG (double hatched).

decays, the differences between $M_{K^-\pi^+\pi^+}$ and $M_{K^-\pi^+}$ are formed for each of the pions, and both are required to be greater than 0.16 GeV/c^2. To remove RCBG, we require that the χ^2 probability of the good vertex fit be greater than 1%, and that the 3D decay-length significance L/σ_L be greater than 3.0. To reject D^+'s from $b\bar{b}$ events, the angle between the D^+ momentum vector and the vertex flight direction is required to be less than 5 mrad in xy and less than 20 mrad in rz. Here we use the angular information instead of the impact-parameter information. We can strongly constrain the D^+ to originate from the IP with the angular information, because of its large decay length.

To form the D^0 vertices, tracks identified as charged kaons, by the requirement that the CRID log-likelihood [17] for the K hypothesis exceeds that for the π hypothesis by at least 3 units, are combined with an opposite-charge track, assumed to be a pion. We use the CRID information for this mode only. To reject background we require x_{D^0} be greater

TABLE I. The number of selected candidates from 1993–1998 SLD experimental data, and contributions from $c\to D$, $b\to D$, and RCBG estimated by MC.

Channel	Candidates	$c\to D$	$b\to D$	RCBG
$D^{*+}\to D^0\pi_s^+$,				
$D^0\to K^-\pi^+$	561	413 (74%)	59 (10%)	89 (16%)
$D^0\to K^-\pi^+\pi^0$	896	601 (67%)	83 (9%)	212 (24%)
$D^0\to K^-\pi^+\pi^+\pi^-$	537	418 (78%)	36 (7%)	83 (15%)
$D^0\to K^-l^+\overline{\nu}$	433	296 (68%)	31 (7%)	106 (24%)
$D^+\to K^-\pi^+\pi^+$	957	698 (73%)	45 (5%)	214 (22%)
$D^0\to K^-\pi^+$	583	403 (69%)	27 (5%)	153 (26%)
Total	3967	2829 (71%)	281 (7%)	857 (22%)

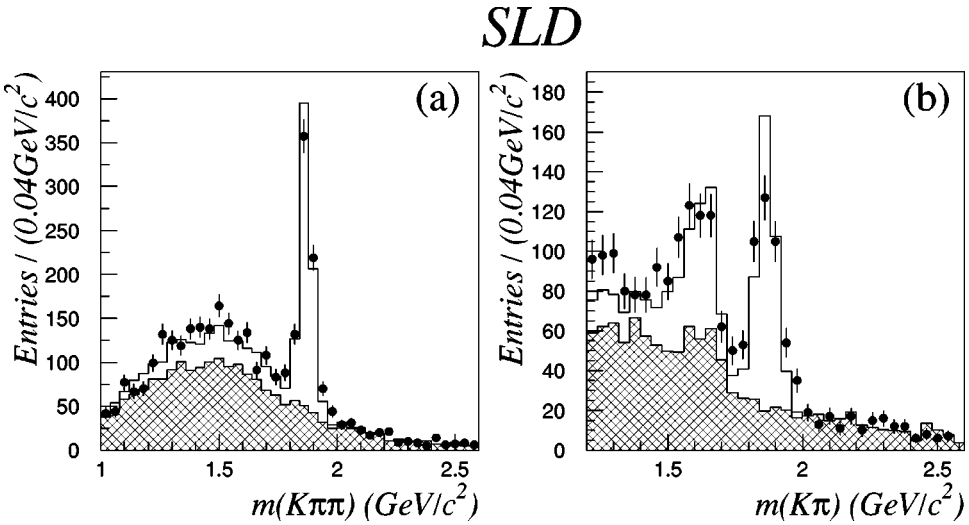

FIG. 3. The mass distributions for (a) D^+ and (b) D^0 mesons. The solid circles indicate the experimental data, and histograms are the MC of signal (open) and RCBG (double hatched). The peaks around $m(K\pi) \sim 1.6$ GeV/c^2 in figure (b) comes from the decay $D^0 \to K\pi\pi^0$.

than 0.4. We require that the vertex fit have χ^2 probability greater than 1% and the 3D decay-length cut L/σ_L be greater than 3.0. To reject the D^0's from D^{*+} decays, the differences between $M_{K^-\pi^+\pi^+}$ or $M_{K^-\pi^+\pi^-}$, and $M_{K^-\pi^+}$ are formed for all other tracks in the same hemisphere, and these are required to be greater than 0.16 GeV/c^2. Finally, to reject D^0's from $b\bar{b}$ events, we require that the xy impact parameter of the D^0 momentum vector relative to the IP be less than 20 μm.

D^+ and D^0 candidates in the ranges of $1.800 < M_{K^-\pi^+\pi^+} < 1.940$ GeV/c^2 and $1.765 < M_{K^-\pi^+} < 1.965$ GeV/c^2, respectively, are regarded as signal. The side-band regions are defined as $1.640 < M_{K^-\pi^+\pi^+} < 1.740$ GeV/c^2 and $2.000 < M_{K^-\pi^+\pi^+} < 2.100$ GeV/c^2 for D^+, and $2.100 < M_{K^-\pi^+} < 2.500$ GeV/c^2 for D^0. In Fig. 3, the invariant mass spectra for the resulting D^+ and D^0 signals are plotted. The backgrounds in the signal regions are estimated from the MC in the same manner as in the D^{*+} analysis.

C. Measurement of A_c

Using the six decay modes, we select 3967 D^{*+}, D^+, and D^0 candidates from 1993–1998 SLD data. The estimated composition is 2829 ± 35 $c \to D$ signal, 281 ± 11 $b \to D$, and 857 ± 19 RCBG. These $c \to D$ signals correspond to a selection efficiency for $c\bar{c}$ events of 3.9%. The results for the number of selected candidates are summarized in Table I.

The charge of the primary c-quark is determined by the charge of the $D^{(*)}$, or K (in the D^0 case). The direction of the primary quark is estimated from the direction of the reconstructed D meson. Figure 4 shows $q \cos\theta_D$ distributions, for the selected D meson sample separately for left- and right-handed electron beams. Here, q is the sign of the charge of the primary c-quark and θ_D is the polar angle of the reconstructed D meson.

To extract A_c, we use an unbinned maximum likelihood fit based on the Born-level cross section for fermion production in Z^0-boson decay. The likelihood function used in this analysis is

$$\ln \mathcal{L} = \sum_{i=1}^{n} \ln\{P_c^j(x_D^i)\cdot[(1-P_eA_e)(1+y_i^2) + 2(A_e-P_e)y_i\cdot A_c^D] + P_b^j(x_D^i)\cdot[(1-P_eA_e)(1+y_i^2) + 2(A_e-P_e)y_i\cdot A_b^D] + P_{RCBG}^j(x_D^i)\cdot[(1+y_i^2) + 2A_{RCBG}y_i]\} \quad (5)$$

where $y = q\cos\theta_D$, n is the total number of candidates, and the index j indicates each of the six charm decay modes.

A_c^D and A_b^D are the asymmetries from D^{*+}, D^+, and D^0 mesons in $c\bar{c}$ and $b\bar{b}$ events, respectively. We treat A_c^D as a free parameter, while A_b^D is fixed. A_b^D is estimated in a similar manner to Ref. [18]. We start with the standard model prediction [19], $A_b = 0.935$, and assign it an error of ± 0.025 from the average value of SLD measurements of 0.911 ± 0.025 [20]. This b-quark asymmetry is diluted by B^0-$\bar{B}^0$ mixing and the wrong-sign D meson from the W^- in $b \to cW^-$, $W^- \to \bar{c}s$ decay. The effective b asymmetry can be expressed by correcting with two dilution factors:

$$A_b^D = A_b \times (1-2\chi_{mixing})(1-2\chi_{W^-\to\bar{c}s}). \quad (6)$$

The value of χ_{mixing} is deduced from the D-meson production rates through B decays. We estimate the $B \to D$ source fractions from MC. Using the fractions and the χ values of $\bar{\chi} = 0.1186 \pm 0.0043$ [20] and $\chi_d = 0.156 \pm 0.024$ [21], we derive the χ_{mixing} value for D^{*+}, D^+, or D^0. The value of $\chi_{W^-\to\bar{c}s}$, the correction for wrong-sign D mesons from the W^- in $b \to cW^-$ decay, is also estimated from MC. We obtain $\chi_{W^-\to\bar{c}s} = 0.023 \pm 0.006$ for the average of D^{*+}, D^+, and D^0 mesons, and 0.021 ± 0.006 for D^{*+} mesons only. Here the errors include the theoretical error of 30% coming from $Br(b \to c\bar{c}s) = 22 \pm 6\%$ [22]. The former and latter $\chi_{W^-\to\bar{c}s}$ values are used for exclusive D reconstruction and inclusive soft-pion analysis, respectively. By combining these two dilutions, we obtain

$$A_b^D = 0.657 \pm 0.025 \quad \text{for} \quad D^{*+},$$

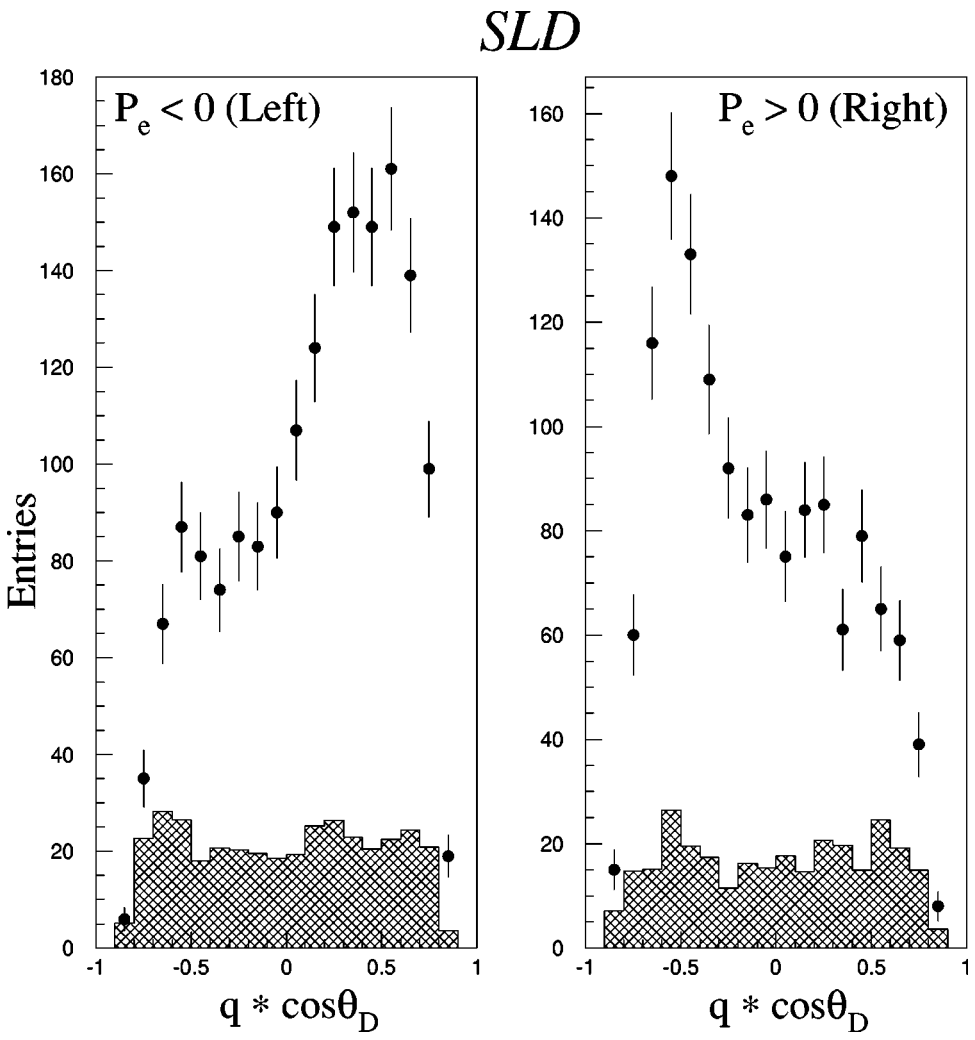

FIG. 4. The distributions of $q \cdot \cos\theta_D$ for the selected D meson sample for (a) left- and (b) right-handed electron beams. The solid circles are experimental data, and double hatched histograms are RCBG estimated from side-band regions.

$= 0.655 \pm 0.026$ for D^+ and

$= 0.762 \pm 0.023$ for D^0.

To check the A_b^D value, we measure A_b^D for D^{*+} using the 1996–1998 experimental data. In this measurement, we select D^{*+} mesons in the decay, $D^{*+} \to D^0 \pi_s^+$ followed by $D^0 \to K^- \pi^+$, $D^0 \to K^- \pi^+ \pi^0$, or $D^0 \to K^- \pi^+ \pi^- \pi^+$. The $b\bar{b}$ events are selected by requiring that the invariant mass for the reconstructed secondary vertices be greater than 2 GeV/c^2 for at least one of the two event hemispheres. In order to select the D^{*+} mesons, we apply similar cuts to those used to select the D^{*+} mesons from c-quarks, but without any xy impact parameter cut to reject D^{*+}'s from b-quarks. We select 2196 D^* candidates with the fractions of 63% $b \to D$, 2% $c \to D$, and 35% RCBG. Using this sample, we measure $A_b^D = 0.58 \pm 0.10$, which is consistent with our assumed A_b^D value for D^{*+}. The error of 0.10 is treated as a systematic error of A_b^D.

We also check the effect of the decay-length cut of the reconstructed D mesons. In this analysis, we apply the decay-length cut of $L/\sigma_L > 1.5 \sim 3.0$ (depending on the charm decay mode) to reject RCBG. This cut may increase the effective value of χ_{mixing}. Using our MC, we estimate the effect of this cut to be small ($\Delta\chi_{mixing}/\chi_{mixing} = 3\%$).

A_{RCBG} is the analog of A_c for the RCBG, and we expect it to be very small. The asymmetry in the side-band region is measured as -0.0006 ± 0.0031, and is assumed to be zero. For A_e, we have taken $A_e = 0.1513 \pm 0.0022$ from the SLD measurement [13].

P_c^j, P_b^j, and P_{RCBG}^j are the probabilities that a candidate from the jth decay mode is a signal from $c\bar{c}$, $b\bar{b}$, or RCBG. The determination of these functions is based on the relative fractions and the x_D distributions for the six decay modes. They are defined as

$$P_c(x_D) = \frac{N_{signal}(x_D)}{N_{total}(x_D)} \cdot \frac{f_c(x_D)}{f_c(x_D) + f_b(x_D)}$$

$$P_b(x_D) = \frac{N_{signal}(x_D)}{N_{total}(x_D)} \cdot \frac{f_b(x_D)}{f_c(x_D) + f_b(x_D)} \qquad (7)$$

$$P_{RCBG}(x_D) = \frac{N_{BG}(x_D)}{N_{total}(x_D)};$$

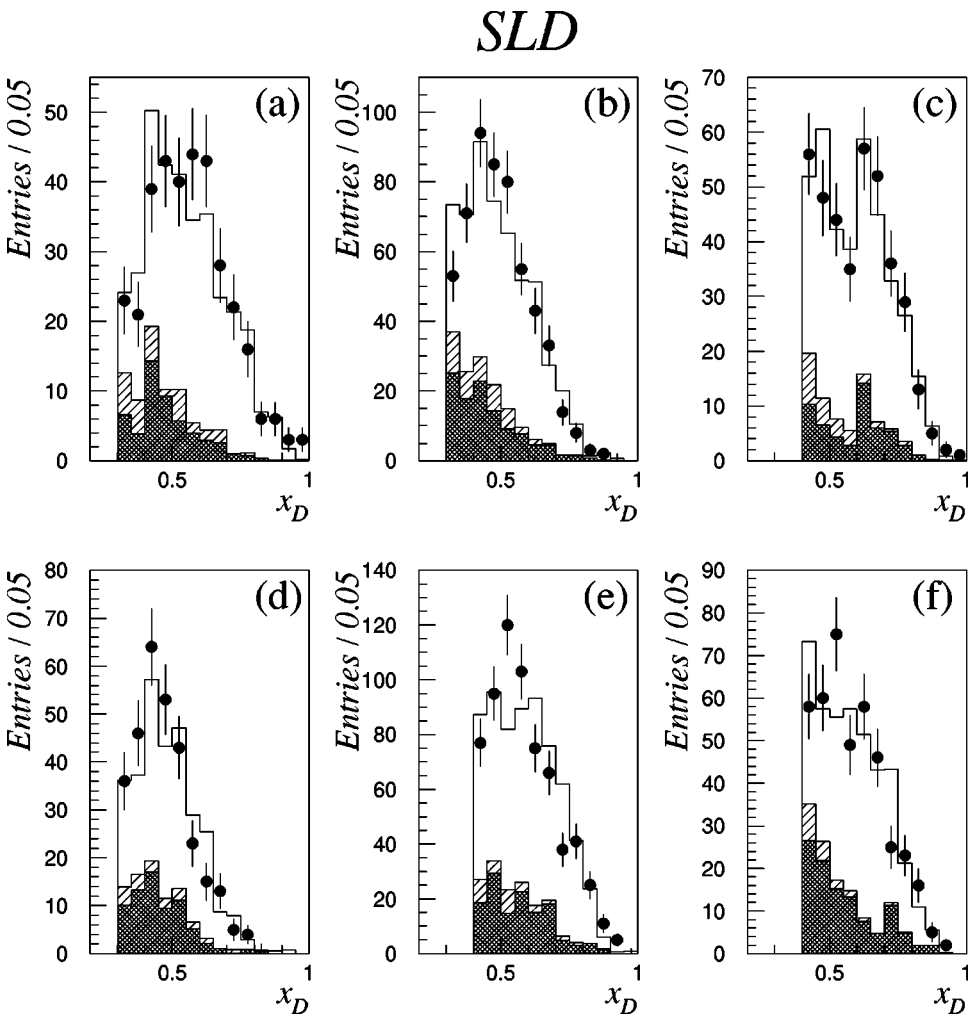

FIG. 5. The x_D distributions for (a) $D^{*+}\to D^0\pi_s^+$, $D^0\to K^-\pi^+$, (b) $D^0\to K^-\pi^+\pi^0$, (c) $D^0\to K^-\pi^+\pi^+\pi^-$, (d) $D^0\to K^-l^+\nu_l(l=\mathrm{e}$ or $\mu)$, (e) $D^+\to K^-\pi^+\pi^+$, and (f) $D^0\to K^-\pi^+$. The solid circles are experimental data and hatched histograms are background estimated from side-band events. MC predictions for D mesons from c-decay (open histograms) and b-decay (single hatched histogram) are also shown.

where $N_{total}(x_D)$ is the observed number of D mesons, and $N_{BG}(x_D)$ is that of background events, in the x_D bin. Using the x_D distributions for the reconstructed D mesons and side-band events, we determine the ratio N_{BG}/N_{total} in each x_D bin. The ratio N_{signal}/N_{total} is given by the relation $N_{signal}/N_{total}=1-N_{BG}/N_{total}$ in each bin. Figures 5(a)–5(f) show the x_D distributions for six decay modes, which are used in this determination.

The functions $f_c(x_D)$ and $f_b(x_D)$ describe the fraction of D mesons in the c and b decays, respectively, and are expressed as

$$f_{c(b)}=\omega_{c(b)}\cdot d_{c(b)}(x_D), \tag{8}$$

where $d_{c(b)}(x_D)$ describes the shape of x_D distributions in $c(b)\to D$, and $\omega_{c(b)}$ represents the total fraction of the $c(b)\to D$ for the reconstructed D candidates. We obtain the function $d_{c(b)}(x_D)$ from MC, and the values of ω_c and ω_b are derived from Table I. The ratio $f_{c(b)}/(f_c+f_b)$ gives the probability that a D candidate is from a primary $c(b)$ quark.

Performing the maximum likelihood fit to the data sample, we measure $A_c=0.671\pm0.096$ (1993–1995) and $A_c=0.681\pm0.047$ (1996–1998). As a check, we also determine A_c with a simple binned fit of the type described in Ref. [16]. We find $A_c=0.731\pm0.102$ (1993–1995) and $A_c=0.666\pm0.049$ (1996–1998); which are consistent with the values above.

D. QCD and QED correction

As a result of hard gluon radiation, the extracted value of $A_{c(b)}$ is somewhat different than its Born-level value in Eq. (1). To account for this, the fit parameter $A_{c(b)}$ in the likelihood function is replaced with the first-order corrected parameter $A_{c(b)}[1-\Delta^{c(b)}_{QCD}(\cos\theta)]$ with $\Delta^{c(b)}_{QCD}(\cos\theta)=C_{c(b)}\Delta^{c(b)}_{QCD,SO}(\cos\theta)$, where $\Delta^{c(b)}_{QCD}$ indicates the magnitude of the leading-order (LO) QCD correction for $c(b)$-quark production, and $\Delta^{c(b)}_{QCD,SO}$ is the LO QCD correction calculated by Stav and Olsen including the quark-mass effect [23]. The factor $C_{c(b)}$ takes into account the mitigation of the effects of gluon radiation due to the analysis procedure. For example, the requirement that D mesons have high x_D values selects against events containing hard gluon radiation, reducing the overall effect of gluon radiation on the observed asymmetry.

The correction factor $C_{c(b)}$ is estimated with the MC program by comparing the effects of QCD radiation, for the JETSET parton shower model, with and without the full analysis including detector simulation:

TABLE II. 1993–1998 average contributions to the estimated systematic error for exclusive D meson reconstruction analysis (left column) and inclusive soft-pion analysis (right column).

Source	δA_c Exclusive $D^{(*)}$	δA_c Inclusive soft pion
Background fraction	0.0111	0.0324
Background acceptance	0.0087	0.0122
Background x_D or P_T^2 distribution	0.0112	0.0018
Background asymmetry	0.0028	0.0093
$f_{b\to D}/(f_{b\to D}+f_{c\to D})$	0.0011	0.0018
$A_{b\to D}$ (A_b)	0.0017	0.0021
$A_{b\to D}$ (Mixing)	0.0092	0.0120
c fragmentation	0.0003	0.0010
b fragmentation	0.0003	0.0005
D meson x_D shape or soft-pion momentum shape	0.0040	0.0003
Polarization	0.0035	0.0033
A_e	0.0002	0.0005
α_s	0.0004	0.0005
Correction factor for first order QCD correction	0.0024	0.0033
Second order QCD correction	0.0006	0.0008
Gluon splitting	0.0002	0.0005
Total	0.0213	0.0383

$$C_q=\frac{A_{q\bar{q}}^{gen}-A_{PS}^{meas}}{A_{q\bar{q}}^{gen}-A_{PS}^{gen}}(q=c,b), \tag{9}$$

where the superscripts ''gen'' and ''meas'' refer to the MC asymmetries for generator level (parton shower model simulation only) and fully analyzed events, respectively. These MC asymmetries are determined by doing a fit to the form

$$A\frac{2\cos\theta}{1+\cos^2\theta} \tag{10}$$

in bins of $\cos\theta$. We obtain $C_c=0.27\pm0.10$ and $C_b=0.17\pm0.08$ for c-quark and b-quark, respectively. Applying the first-order QCD correction with the correction factors $C_{c(b)}$, leads to a 1.0% increase of A_c.

In this analysis, we have also considered the effects of next-to-leading order (NLO) gluon radiation. The NLO QCD correction is written as

$$\Delta_c^{O(\alpha_s^2)}=\left(\frac{\alpha_s}{\pi}\right)^2\times4.4\times C_c+\Delta_{gs} \tag{11}$$

where the first term is from hard gluon emission [24]. We use the same correction factor C_c as in Eq. (9). The second term Δ_{gs} accounts for the effects of the process $g\to c\bar{c}$ for gluons which arise during the shower and fragmentation processes.

The effects of gluon splitting have been taken into account by analyzing the MC as if it were data, with and without events with gluon splitting. The resulting difference must be scaled to account for the difference between the JETSET gluon splitting rates and the currently measured values for these rates. The rate for gluon splitting to charm quark pairs in JETSET is 0.0136 per hadronic event, and the current CERN e^+e^- collider LEP average [20] is 0.0319 ± 0.0046, yielding a scale factor of 2.35 ± 0.34.

The second-order QCD correction increases A_c by 0.4%. Applying the first- and second-order QCD corrections, we obtain $A_c=0.681\pm0.097$ (1993–1995) and $A_c=0.690\pm0.047$ (1996–1998).

Using ZFITTER(6.23) [19], we estimate QED corrections including initial- and final-state radiation, vertex correction, γ exchange, and γ-Z interference. We use the input values $m_{top}=175$ GeV/c^2 and $m_{Higgs}=150$ GeV/c^2. These corrections increase A_c by 0.2%. Applying the QED corrections, we obtain $A_c=0.682\pm0.097$ (1993–1995) and $A_c=0.691\pm0.047$ (1996–1998).

E. Systematic errors

The following systematic errors have been estimated and are summarized in Table II:

The largest uncertainties are due to the RCBG, arising from the statistics of the MC and side-band events, which are used to determine the fraction of the RCBG in the signal, and the shape of RCBG x_D distribution which is determined by side-band events. The uncertainty of the RCBG x_D shape is estimated by comparing the x_D distributions for MC RCBG events and for side-band events.

There is a difference in acceptance between signal and RCBG event samples. In this analysis, we determine the RCBG probability function as a function of x_D. This is correct if the ratio between the signal and RCBG acceptance is constant over the different $\cos\theta$ regions. In order to study this, we compare the RCBG $|\cos\theta|$ distribution obtained from the side-band region and that from the signal region events weighted by the RCBG probability function

$P_{RCBG}(x_D)$ in Eq. (5). These two distributions become significantly different starting at $|\cos\theta|\sim 0.65$. Hence, we apply an acceptance cut of $|\cos\theta_D|<0.65$, then regard the difference between with and without the cut as a systematic uncertainty.

We expect the asymmetry of RCBG to be very small, and take a central value of $A_{RCBG}=0$. Since the asymmetry of the side-band events is measured to be -0.0006 ± 0.0031, we take -0.0037 as a lower limit on A_{RCBG}.

We vary $f_{b\to D}/(f_{b\to D}+f_{c\to D})$, the fraction of D mesons from $Z^0\to b\bar{b}$, by $\pm 20\%$ to account for differences between our MC and the range of measurements of $D^{(*)+}$ production in Z^0 decay [18,25].

The effect of the uncertainty of A_b^D is estimated by varying $\delta A_b^D=\pm 0.10$, where the error is from the statistical error of our A_b^D measurement by using experimental data. In Table II, we show the resultant error in A_c coming from the uncertainty in $A_b(0.935\pm 0.025)$ separately from the uncertainty in the mixing parameter.

The systematic error on the fragmentation function is estimated by modifying the x_D distributions in heavy-quark fragmentation. In our MC sample, we use Peterson fragmentation and the average x_D values are $\langle x_D\rangle=0.508$ and 0.318 for $c\to D$ and $b\to D$, respectively. We change the values by $\Delta\langle x_D\rangle=\pm 0.015(\pm 0.010)$ for $c(b)\to D$.

Our sensitivity to the RCBG x_D distribution is checked by performing the analysis with P_{RCBG} derived from the MC background instead of the data side-bands.

The shapes of the x_D distributions in $c(b)\to D$, expressed as $d_{c(b)}(x_D)$ in Eq. (8), are obtained by fitting to the MC x_D distributions. The sensitivity to this procedure is checked by performing the analysis with a binned MC x_D distribution.

We assume $A_e=0.1513\pm 0.0022$, and estimate this systematic error by varying A_e within the error. The precision of the polarization measurements are $\Delta P_e=1.1\%$ (1993), 0.5% (1994–1995), and 0.4%(1996–1998) [12,13]. We estimate the systematic error due to polarization uncertainties by varying P_e with these errors.

We consider two sources of uncertainties on the leading order QCD correction: The uncertainty on α_s and the uncertainty in the estimation of the correction factor due to the analysis bias. The range of α_s chosen for the analysis is 0.118 ± 0.007, while that for the correction factor is 0.27 ± 0.10 for c quark or 0.17 ± 0.08 for b quark, as described in Sec. III D.

In order to estimate the hard-gluon-radiation uncertainty in the second-order QCD correction, we vary the magnitude of the correction by 50% of itself. We use the experimental error for the uncertainty in gluon splitting into $c\bar{c}$.

The total systematic errors are 0.034 and 0.021 for 1993–1995 and 1996–1998 SLD runs, respectively.

F. Results

We obtain the following results for the measurements using exclusive channels: $A_c=0.682\pm 0.097(\text{stat.})\pm 0.034(\text{syst.})$ (1993–1995) and $A_c=0.691\pm 0.047(\text{stat.})\pm 0.021(\text{syst.})$ (1996–1998). The combined result is

$$A_c=0.690\pm 0.042(\text{stat.})\pm 0.021(\text{syst.}).$$

IV. INCLUSIVE SOFT-PION ANALYSIS

In this analysis, c quarks are identified by the presence of soft pions from the decay $D^{*+}\to D^0\pi_s^+$. Since this decay has a small Q value of $m_{D^*}-m_{D^0}-m_\pi=6$ MeV/c^2, the maximum transverse momentum of the π_s with respect to the D^{*+} flight direction is only 40 MeV/c.

A. Jet reconstruction and soft-pion selection

We select hadron events and reject $b\bar{b}$ events by using the same criteria described in Sec. II. The D^{*+} flight direction is approximated by the jet direction, where charged tracks and neutral clusters are clustered into jets, using an invariant-mass (JADE) algorithm. In the jet clustering, particles are merged together in an iterative way if their invariant mass is less than 4.6 GeV/c^2. We only use the tracks and clusters which have the momentum of greater than 1.2 GeV/c and 1.0 GeV/c, respectively, to form the jet. The tracks are required to satisfy the track quality cuts described in Sec. II and to have vertex hits.

The jets must satisfy the following criteria:

(1) At least 3 charged tracks;

(2) At least one track with momentum P>5 GeV/c;

(3) The net charge of the jet, Σq, should be $|\Sigma q|\leqslant 2$;

(4) Sum of the largest and second largest 3D normalized impact parameters of the tracks >2.5 σ; and

(5) There is at least one opposite-charged-track pair which has χ^2 probability of two tracks coming from the same vertex greater than 1%.

The criteria (2) and (3) are effective to reduce the huge RCBG. The criterion (4) rejects the light flavor events. The criterion (5) relies on the fact that it is likely that the D^0 decays into at least one pair of oppositely charged tracks.

After selecting the jet candidates, we look for the soft-pions using a momentum cut of $1<P<3$ GeV/c and an impact-parameter cut of less than 2σ from the IP. Since soft-pions in $c\bar{c}$ events have much higher momentum than those in $b\bar{b}$ events, the former criterion rejects such soft-pions from $b\bar{b}$ events. The latter criterion is also effective to reduce the soft-pions from $b\bar{b}$, because D^* decays from $b\bar{b}$ events have significant transverse momentum relative to the parent B flight direction, and they do not appear to originate from the primary vertex due to the B lifetime.

Using the selected soft-pion candidates, the momenta transverse to the jet axis. P_T, are calculated. Figure 6(a) shows the P_T^2 distribution for the soft-pion candidate tracks. The peak around $P_T^2=0$ is from charm signal. We define $P_T^2<0.01$ $(\text{GeV}/c)^2$ as the signal region, where a signal-to-background ratio of 1:2 is observed. From 1993–1998 data, 12992 soft-pion candidates are selected in the region.

B. BG determination and A_c measurement

To evaluate the number of the $D^{*+}\to D^0\pi_s^+$ decays, a fit to the observed P_T^2 distribution is performed using the signal plus background shape. The signal shape is assumed to be a simple exponential

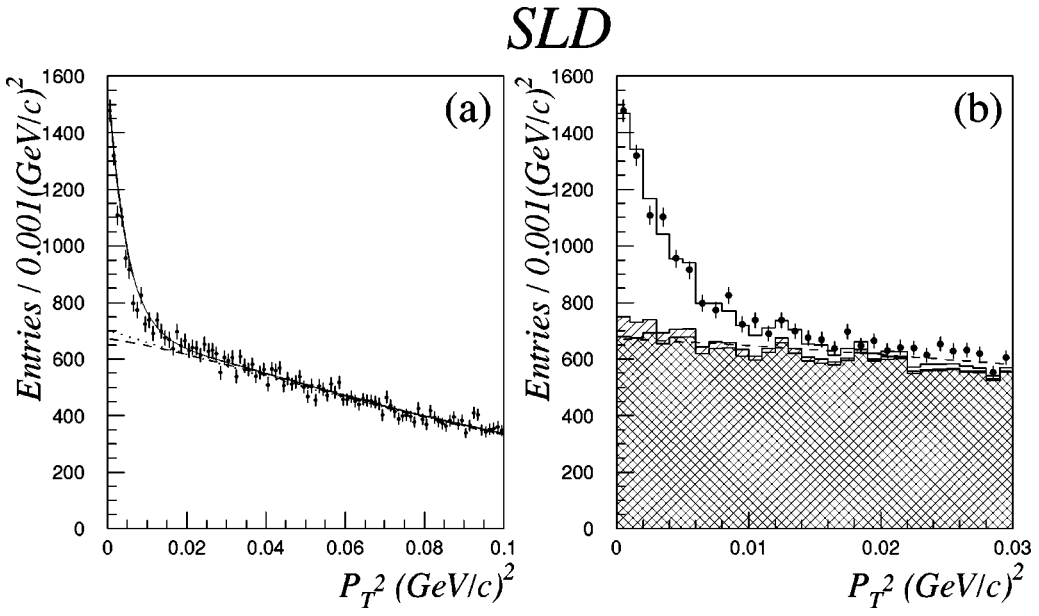

FIG. 6. The P_T^2 distributions for soft-pion candidate tracks. (a) The solid circles indicate the experimental data. The curves are the result of the a fit $S(P_T^2)+F_1(P_T^2)$ performed for $P_T^2<0.1$ GeV/c (solid line), and the extrapolations of $F_1(P_T^2)$ (dashed line) and $F_2(P_T^2)$ (dotted line). The definition of the functions are described in the text. (b) The solid circles are the experimental data, and histograms are MC predictions for D mesons from c-decay (open), D mesons from b-decay (single hatched), and background (double hatched). The extrapolation of $F_1(P_T^2)$ is also shown as a dashed line.

$$S(P_T^2)=\alpha\exp(-P_T^2/\beta).$$

We obtain $\beta=0.00471\pm0.00007$ by fitting the MC spectrum of $D^{*+}\to D^0\pi_s^+$ decays and fix the value of β to fit the experimental data. For the background shape, we try two kinds of functions with three free parameters each:

$$F_1(P_T^2)=a/(1+bP_T^2+c(P_T^2)^2),$$

$$F_2(P_T^2)=a'+b'\exp(-P_T^2/c').$$

The fit results are illustrated in Fig. 6(a), where we show the extrapolation of $F_1(P_T^2)$ (dashed line) and $F_2(P_T^2)$ (dotted line).

The observed signal in 1993–1998 data is 4291 ± 147 (χ^2/ndf$=219.0/196$) with $S(P_T^2)+F_1(P_T^2)$ and 4032 ± 124 (χ^2/ndf$=224.0/196$) with $S(P_T^2)+F_2(P_T^2)$, where the fit is performed in each case for $P_T^2<0.1$ GeV/c. We choose $F_1(P_T^2)$ for the background shape to measure the A_c, because of its smaller χ^2/ndf value. The difference between these two functions is regarded as a systematic error.

We determine the relative normalizations of signal and background for the MC prediction using the above fit to the data. Figure 6(b) shows the detailed P_T^2 distribution from the MC prediction with this normalization. We also overlay the background shape extrapolated by the fitting with $S(P_T^2)+F_1(P_T^2)$ (dashed line). Using the MC, we estimate the contributions of $c\to D^{*+}$ and $b\to D^{*+}$ as 3791 ± 39 and 500 ± 14, respectively, in 1993–1998 data.

In order to ensure that there is little room for non-D^* sources of slow pions in the data, we compared the signal obtained by fitting to the experimental data and the number of D^*'s expected by MC. Here normalization of the MC is determined by the number of hadronic events. Using MC, we estimate the number to be 4507 ± 57. Comparing this number and the obtained experimental number of 4291 ± 147, we conclude that other charm-decay sources in the experimental data are small.

The direction of the primary quark is estimated from the jet axis, and the charge of the primary c quark is determined by the charge of the π_s. Figure 7 shows the $q\cos\theta_D$ distributions, where q is the sign of the primary c-quark, and θ_D is the polar angle of the jet axis, for the selected D^{*+} sample separately for left- and right-handed electron beams.

To extract A_c, we use an unbinned maximum likelihood fit, using a likelihood function similar to the exclusive D reconstruction analysis [Eq. (5)]. We regard the A_c as a free parameter, and fix the asymmetry of D^{*+} from $b\bar{b}$ events, A_b^D. This value is obtained by following the similar procedure described in Sec. III C.

We expect the asymmetry for the BG, A_{BG}, to be very small and assume it to be zero. Using the MC, we measure the asymmetry of the background to be 0.009 ± 0.017.

For the probabilities P_c, P_b, and P_{RCBG} in Eq. (5), we used the following functions:

$$P_c(P,P_T^2)=\frac{N_{signal}(P,P_T^2)}{N_{total}(P,P_T^2)}\cdot\frac{f_c(P)}{f_c(P)+f_b(P)}$$

$$P_b(P,P_T^2)=\frac{N_{signal}(P,P_T^2)}{N_{total}(P,P_T^2)}\cdot\frac{f_b(P)}{f_c(P)+f_b(P)} \quad (12)$$

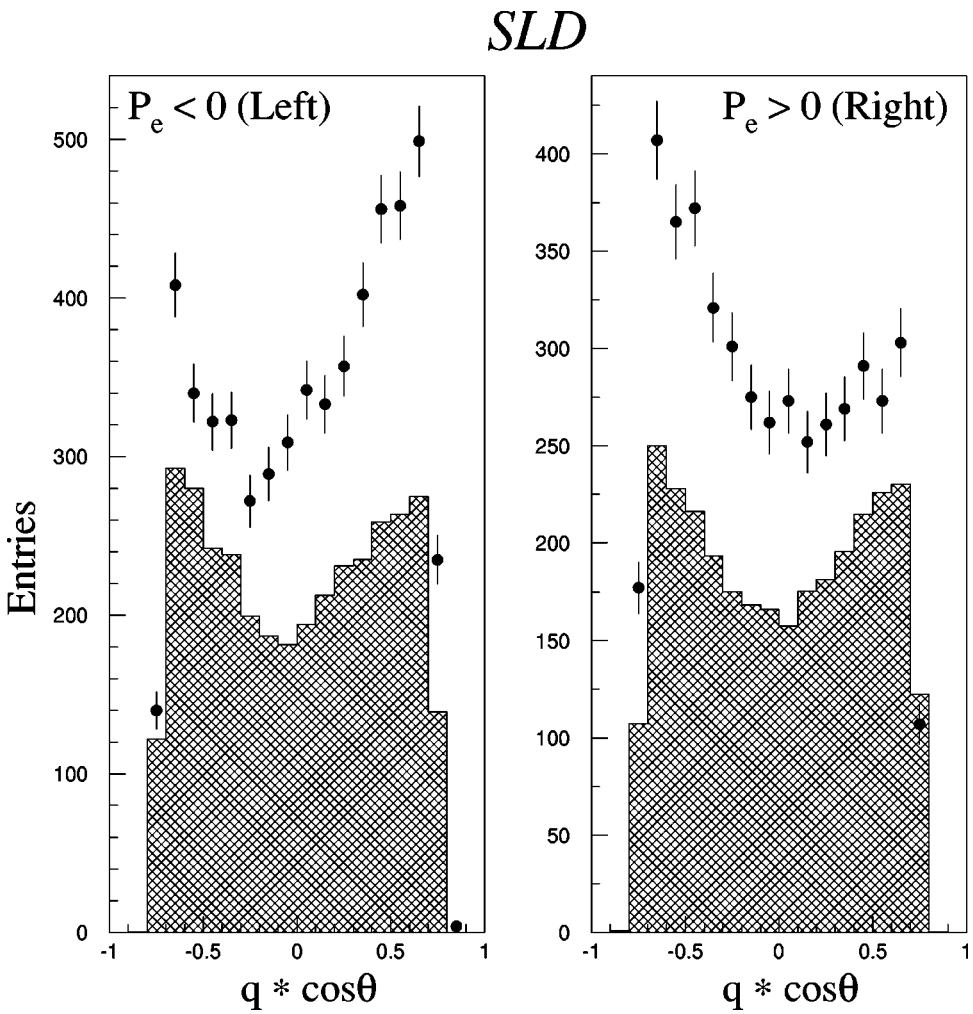

FIG. 7. The distributions of $q\cdot\cos\theta_D$ for the selected D^{*+} meson sample for (a) left- and (b) right-handed electron beams. The solid circles are experimental data, and hatched histograms are RCBG estimated from side-band regions.

$$P_{RCBG}(P,P_T^2)=\frac{N_{BG}(P,P_T^2)}{N_{total}(P,P_T^2)};$$

where P and P_T^2 indicate the momentum and the squared transverse momentum to the D^* jet axis for soft-pion tracks, respectively. N_{total} and N_{BG} are the observed number of soft-pion candidates and that of background in each P and P_T^2 bin, respectively. We estimate N_{BG} from MC, and the relation $N_{signal}/N_{total}=1-N_{BG}/N_{total}$ gives the ratio N_{signal}/N_{total}. Figure 8 shows the momentum distributions for experimental data and MC predictions. Figures 6 and 8 are used for this estimation.

The function $f_{c(b)}$ in Eq. (12) describes the fractions of D mesons in the $c(b)$ decays, and the ratio $f_{c(b)}/(f_c+f_b)$ gives the probability that D candidate is from a primary $c(b)$ quark. We regard $f_{c(b)}$ as a function of soft-pion momentum, P. The function is expressed as $f_{c(b)}=\omega_{c(b)}\cdot d_{c(b)}(P)$. Here $d_c(b)$ is determined by the shape of MC soft-pion momentum distributions in $c(b)\to D$ and $\omega_{c(b)}$ is the estimated total fraction of the $c(b)\to D$ among the selected candidates.

Performing the maximum likelihood fit to the data sample, we measure $A_c=0.654\pm0.125$ (1993–1995) and $A_c=0.673\pm0.056$ (1996–1998). As a check, we also measure A_c with a simple binned fit as $A_c=0.520\pm0.164$ (1993–1995) and $A_c=0.665\pm0.085$ (1996–1998), which are consistent with the above values.

The first- and second-order QCD correction and QED correction are applied with the same method as in the exclusive D reconstruction analysis. In the QCD correction, the correction factor due to the analysis bias is estimated as $C_c=0.40\pm0.14$ for c quark and $C_b=0.19\pm0.09$ for b quark. Applying the first- and second-order QCD correction with this factors, and QED correction, we obtain $A_c=0.669\pm0.127$ (1993–1995) and $A_c=0.689\pm0.057$ (1996–1998).

C. Systematic errors

The estimated uncertainties in this analysis are summarized in Table II, where we show average systematic errors for the 1993–1998 data. In the soft-pion analysis, we use the same procedures to estimate the systematic errors as those in the exclusive $D^{(*)}$ reconstruction analysis in many sources. Here we only explain error sources where we take a different method.

The largest uncertainties are due to the imperfect knowledge of the background fraction and its shape. The background is determined by fitting to the P_T^2 distribution of the experimental data, and we try two functions F_1 and F_2 de-

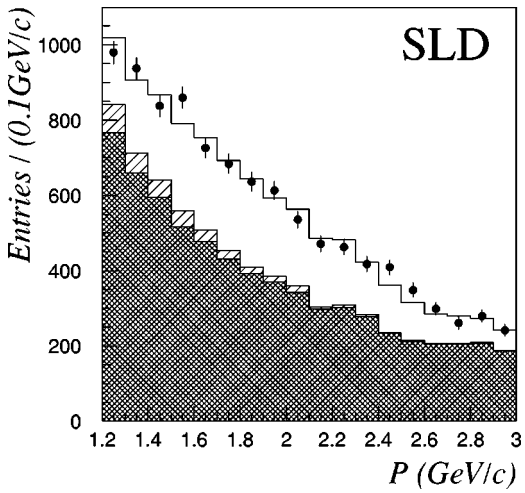

FIG. 8. The momentum distribution for soft-pion candidate tracks. The points are experimental data. The histograms are MC predictions of D's from c decays (open), D's from b decays (single hatched), and background (double-hatched).

scribed above. In order to estimate the background fraction uncertainty, we fix the background shape as F_1, and change its height so as to cover the possible range of the background fraction. The background shape uncertainty is estimated by using the two background shapes, F_1 and F_2, while keeping the integrated number of the background events in the signal region $[P_T^2<0.1\ \ (\mathrm{GeV}/c)^2]$ constant.

The shape of the soft-pion momentum distributions in $b\to D^*$ or $c\to D^*$ is determined by fitting to the MC distributions. The uncertainty concerning this distribution is estimated by performing the analysis using a binned momentum distribution instead of fitting.

The total systematic errors are obtained to be ± 0.067 and ± 0.053 for 1993–1995 and 1996–1998, respectively.

D. Results

The A_c values obtained in the inclusive soft-pion analysis are $A_c=0.669\pm 0.127(\mathrm{stat.})\pm 0.067(\mathrm{syst.})$ (1993–1995) and $A_c=0.689\pm 0.057(\mathrm{stat.})\pm 0.053(\mathrm{syst.})$ (1996–1998). The combined result is

$$A_c=0.685\pm 0.052(\mathrm{stat.})\pm 0.038(\mathrm{syst.}).$$

V. CONCLUSION

Using the 1993–1998 experimental data collected by the SLD experiment, we measure the parity-violation parameter A_c using two different c-quark tagging methods:

$$A_c=0.690\pm 0.042(\mathrm{stat.})\pm 0.019(\mathrm{syst.}) \quad \text{and}$$

$$A_c=0.685\pm 0.052(\mathrm{stat.})\pm 0.036(\mathrm{syst.}),$$

from exclusive charmed-meson reconstruction and inclusive soft-pion analysis, respectively.

To combine them, we must avoid double counting signal events from both samples. We find that 1182 events are common to the two analyses. The statistical error for the soft-pion analysis without the overlapping events is ± 0.061. The combined result is

$$A_c=0.688\pm 0.041,$$

where we have also treated the common systematic errors as fully correlated.

The result is consistent with the standard model prediction of 0.667, obtained by using ZFITTER(6.23) [19] with a top-quark mass of 175 GeV/c^2 and a Higgs boson mass of 150 GeV/c^2. This measurement tests the Z^0 to c quarks coupling to 6% accuracy. Because of the presence of electron polarization, we can measure A_c directly, with very little dependence on A_e. Therefore this measurement has much less dependence of the weak-mixing angle than the forward-backward asymmetry measurements. This result represents the currently most precise measurement of A_c.

ACKNOWLEDGMENTS

We thank the personnel of the SLAC accelerator department and the technical staffs of our collaborating institutions for their outstanding efforts on our behalf. This work was supported by the Department of Energy; the National Science Foundation; the Istituto Nazionale di Fisica Nucleare of Italy; the Japan-U.S. Cooperative Research Project on High Energy Physics; and the Science and Engineering Research Council of the United Kingdom.

[1] SLD Collaboration, K. Abe *et al.*, Phys. Rev. Lett. **75**, 3609 (1995).

[2] SLD Collaboration, K. Abe *et al.*, Phys. Rev. Lett. **83**, 3384 (1999).

[3] ALEPH Collaboration, R. Barate *et al.*, Phys. Lett. B **434**, 415 (1998); ALEPH Collaboration, D. Decamp *et al.*, *ibid.* **263**, 325 (1991); DELPHI Collaboration, P. Abreu *et al.*, Eur. Phys. J. C **10**, 219 (1999); L3 Collaboration, O. Adriani *et al.*, Phys. Lett. B **292**, 454 (1992); OPAL Collaboration, G. Alexander *et al.*, Z. Phys. C **73**, 379 (1997); OPAL Collaboration, G. Alexander *et al.*, *ibid.* **70**, 357 (1996).

[4] SLD Collaboration, K. Abe *et al.*, Phys. Rev. D **53**, 1023 (1996).

[5] M. Hildreth *et al.*, Nucl. Instrum. Methods Phys. Res. A **367**, 111 (1995).

[6] C. J. S. Damerell *et al.*, Nucl. Instrum. Methods Phys. Res. A **288**, 288 (1990).

[7] K. Abe *et al.*, Nucl. Instrum. Methods Phys. Res. A **400**, 287 (1997).

[8] SLD Collaboration, T. Abe, Nucl. Instrum. Methods Phys. Res. A **447**, 90 (2000).

[9] D. Axen *et al.*, Nucl. Instrum. Methods Phys. Res. A **328**, 472

(1993).
[10] A. C. Benvenuti *et al.*, Nucl. Instrum. Methods Phys. Res. A **290**, 353 (1990).
[11] K. Abe *et al.*, Nucl. Instrum. Methods Phys. Res. A **343**, 74 (1994).
[12] SLD Collaboration, K. Abe *et al.*, Phys. Rev. Lett. **73**, 25 (1994); **78**, 2075 (1997).
[13] SLD Collaboration, K. Abe *et al.*, Phys. Rev. Lett. **84**, 5945 (2000).
[14] SLD Collaboration, K. Abe *et al.*, Phys. Rev. D **53**, 1023 (1996).
[15] SLD Collaboration, K. Abe *et al.*, Phys. Rev. Lett. **80**, 660 (1998); D. Jackson, Nucl. Instrum. Methods Phys. Res. A **388**, 247 (1997).
[16] SLD Collaboration, K. Abe *et al.*, Phys. Rev. Lett. **74**, 2895 (1995).
[17] SLD Collaboration, K. Abe *et al.*, Phys. Rev. D **59**, 052001 (1999).
[18] OPAL Collaboration, R. Akers *et al.*, Z. Phys. C **60**, 601 (1993); ALEPH Collaboration, D. Buskulic *et al.*, *ibid.* **62**, 1 (1994).
[19] D. Bardin *et al.*, Report No. CERN-TH-6443-92, 1992.
[20] The LEP Collaborations, the LEP Electroweak Working Group, and the SLD Heavy Flavor and Electroweak Groups, CERN-EP/2000-016, 2000.
[21] Particle Data Group, C. Caso *et al.*, Eur. Phys. J. C **3**, 1 (1998).
[22] M. Neubert and C. T. Sachrajda, Nucl. Phys. **B483**, 339 (1997); W. F. Palmer and B. Stech, Phys. Rev. D **48**, 4174 (1993).
[23] J. Stav and H. Olsen, Phys. Rev. D **52**, 1359 (1995); **54**, 817 (1996).
[24] G. Altarelli and B. Lampe, Nucl. Phys. **B391**, 3 (1993).
[25] DELPHI Collaboration, P. Abreu *et al.*, Z. Phys. C **59**, 533 (1993).